

MRI Features of Different Molecular subtypes of Breast Cancer

Research Article

Issar P¹, Sinha S², Ravindranath M³ and Issar SK⁴

¹Department of Radiodiagnosis, JLN Hospital and Research Centre, India

²Department of Radiodiagnosis, KIMS Superspeciality Hospital, India

³Department of Pathology, JLN Hospital and Research Centre, India

⁴Director In-charge, JLN Hospital and Research Centre, India

*Corresponding author: Issar P, HOD Radiodiagnosis, JLN Hospital and Research Centre Bhilai Chhattisgarh, DB-8, Talpuri, Bhilai, Chhattisgarh, 490009, Tel: 9407983540; Email: mareesh_23@yahoo.co.in

Copyright: © 2020 Issar P, et al. This is an open access article distributed under the Creative Commons Attribution License, which permits unrestricted use, distribution, and reproduction in any medium, provided the original work is properly cited.

Article Information: Submission: 25/06/2020; Accepted: 04/09/2020; Published: 10/09/2020

Abstract

Background: Molecular subtypes of breast cancer have different imaging findings on MRI.

Aim: To assess the MRI features of different molecular subtypes of breast cancer.

Setting and Design: A retrospective observational study.

Materials and Methods: 82 patients with histopathologically confirmed breast cancer along with immunohistochemistry were included in this study. MRI was performed with a 1.5 T Scanner (Signa excite GE healthcare) using a dedicated 8 channel breast coil. MRI findings were correlated with the different molecular subtypes of breast cancer. Statistical Analysis was performed with statistical software SPSS 17.0, p-Value < 0.05 were considered significant.

Results: The molecular subtypes distribution was Luminal A in 48.78%, Luminal B in 9.76%, Human Epidermal Receptor 2 positive (HER2+) in 14.64% and Triple Negative Breast Cancer (TNBC) in 26.82% of the patients. Luminal A subtype presented mainly as a mass lesion with an irregular shape, spiculated margin, and heterogeneous enhancement. TNBC was mainly showing high intratumoral signal intensity (p=0.0003), unifocal lesion (p=0.0002), round or oval (p=0.006), smooth margin, rim enhancement and having high ADC value (p=0.017). Multifocal or non-mass lesion along with axillary adenopathy, skin, peritumoral, and prepectoral edema was found to be more common in Luminal B and HER2+ subtypes.

Conclusion: Breast MR Imaging can help in assessing different molecular subtypes of breast cancer, especially in Luminal A, as an irregular mass with spiculated margin and round or oval mass with rim enhancement and high ADC value in TNBC. Multifocal masses with adenopathy and skin involvement in Luminal B and HER2+ molecular subtypes.

Keywords: Breast MRI; HER 2 positive; Luminal A; Luminal B; Triple negative Breast cancer.

Introduction

Breast cancer is a heterogeneous disease with many histological and molecular subtypes that have a different response to therapy and prognosis. Traditional criteria for treatment choices were the size of the tumor, histological grade, lymph node involvement, local invasion, and distant metastasis. However, patients with the same stage of cancer and similar histopathological characteristics may

show different clinical behavior and prognosis. Advances in gene expression analysis with DNA microarray technology have provided new molecular subtypes. Luminal A, Luminal B, Human epidermal growth factor receptor 2 (HER2) enriched & triple-negative (basal-like). Immunohistochemical (IHC) staining is a reliable surrogate for these subtypes [1,2]. Luminal A subtype is associated with a low proliferation index (Ki-67), accounts for 50-60% of all breast cancers,

and has the best prognosis. Luminal B subtype is associated with a high expression of the Ki-67 proliferation index, accounting for 20 % of all breast cancer, and has a poor prognosis as compared to Luminal A. Luminal B characteristically do not over express HER2/neu, but approximately 30% of them will be HER2 enriched. HER2+ subtypes account for 10% of all breast cancers and are characterized by the absence of hormone receptors and high expression of the HER2/neu gene. Triple-negative subtype accounts for 7-16% of all breast cancers and is characterized by the absence of expression of hormone receptors and HER2+, associated with a high expression of cytokeratin genes of high molecular weight. This subtype is associated with less differentiated invasive carcinoma and accounts for 70% of breast cancers on BRCA 1 mutated females. HER2+ and Triple-negative subtypes show a good response to chemotherapy but have the worst overall survival [3-5].

Dynamic contrast-enhanced magnetic resonance imaging (DCE-MRI) is an efficient imaging technique in evaluating breast cancer patients for preoperative surgical planning and treatment choices. The correlation of imaging findings with molecular subtypes of breast cancer is an emerging area of recent studies. The purpose of this study was to assess the MRI features of different molecular subtypes of breast cancer.

Materials and Methods

This retrospective MRI study included 82 women with pathologically confirmed breast cancer and different molecular subtypes by immunohistochemistry from March 2018 to February 2020. Molecular subtype findings based on immunohistochemistry were correlated with MR findings.

Patients having ductal carcinoma in situ & those who had received neoadjuvant therapy were excluded from the study.

Methods

MR images were obtained with the patient in prone position in a 1.5 T scanner (Signa Excite GE Healthcare, Milwaukee) using a dedicated 8 channel breast coil. Each study includes pre-contrast as well as post-contrast sequence. All MRI sequences and parameters are listed in Table 1. Diffusion-weighted imaging (DWI) at b values 0 and 1000 was performed and Apparent Diffusion Coefficient (ADC) was calculated. Single unenhanced and six serial dynamic contrast-enhanced axial image set was obtained using VIBRANT acquisition

Table 1: Breast MRI sequence and parameters

Sequences	TR(ms)	TE(ms)	FOV (mm)	Matrix	Slice thickness (mm)	Intersection gap (mm)
Ax T1	550	15.9-25.8	360x360	320x256	4.0	0.0
Ax T2	6075	120	360x360	320x256	4.0	0.0
Ax T2 FAT SAT	3900	850	360x360	320x256	4.0	0.0
Ax DWI b 0 & 1000	1850	68.2	360x360	256x192	4.0	0.0
Pre contrast Ax Vibrant	6.1	2.9	360x360	350x224	2.2	0.0
Ax Vibrant Multiphase	6.1	2.9	360x360	350x224	2.2	0.0

technique before and immediately after rapid I.V bolus infusion of 0.1 mmol/Kg body weight of gadodiamide (Omniscan) at a rate of 2 ml/sec with a power injector. Immediately following the contrast injection, 20c.c. saline was injected to flush all contrast media. Dynamic contrast-enhanced image acquisition was started just after the injection. The acquisition time of each phase was 80 seconds. The total duration of the MRI was 25 minutes. Subtraction and maximum intensity projection (MIP) sequences were generated.

Image analysis

MR images were retrospectively interpreted by two radiologists (PI, SS) having 11 and 5 years experienced in breast MRI. Any disagreement was solved by consensus. The morphological and enhancement kinetic features were analyzed based on the 5th Edition of the American College of Radiology (ACR) breast imaging reporting and data system (BI-RADS) MR lexicon [6]. The morphology included mass and non-mass type lesions. When a breast had more than one lesion and those lesions were not connected, it was categorized as having multiple lesions. The non-mass enhancement was further described as linear, ductal, segmental, and regional. The evaluation of the enhancement kinetic curve was based on the initial phase (within the first 2 minutes) and the late phase (after 2 minutes). The initial enhancement phase is further categorized into fast, medium, and slow. The late enhancement phase was described as persistent, plateau, and washout. On this basis, the tumor was graded with 1,2, and 3 enhancement kinetics. For the measurement of tumor size, the longest dimension of the tumor appearing on the post-contrast scan was recorded. When there were multiple lesions in one breast, only the biggest lesion was measured. Additionally, in mass lesions, whether they were showing rim enhancement pattern, were evaluated. The vessel enhancement could be easily identified and excluded based on MIP. Axillary lymph nodes were evaluated on pre-contrast non FAT SAT axial, T1 Weighted Imaging (WI). An enlarged lymph node was defined as a node, abnormal in shape (round or oval) with irregular margin, increased cortical thickness (greater than 3mm), completely or partially effaced fatty hilum [7]. It was considered as suspicious of Malignancy and confirmed on pathological examination of specimen received with axillary node dissection.

MRI features of different molecular subtypes were compared for tumor size, shape, and margin, intratumoral signal intensity on T2WI, Dynamic Contrast Enhancement (DCE) pattern, signal intensity curve, and multifocal or multicentric disease. We analyzed all lesions for associated MR Imaging findings such as skin or nipple invasion, chest wall, or pectoralis muscle invasion. These were described as abnormal enhancement of these locations. Edema if present, was sub-classified as skin edema, perilesional edema, and prepectoral edema. Statistical analysis was performed by using statistical software SPSS 17.0, p<0.05 was considered significant.

Histopathologic Assessment

Histopathologic analysis from the surgical specimen, revealing histological type, pathological grade, and lymph node status was obtained. The molecular subtype of breast cancer was classified depending on the status of ER, PR, HER 2, and Ki67 index (Table 2). HER 2 status was scored as 1+, 2+, or 3+ using IHC analysis, as well as

fluorescence in situ hybridization (FISH). If the score performed 2+ for IHC, a positive HER 2 result was IHC staining of 3+ or 2+ with a FISH result confirmed gene amplification.

Statistical Analysis

Statistical Analysis was performed with statistical software SPSS 17.0, p-Value < 0.05 were considered significant. The study was approved by the institutional ethical committee and informed consent was waived due to the retrospective design of the study.

Results

The study includes 82 breast cancer women with ages ranged from 32 to 80 years. Breast cancer was classified into molecular subtype as Luminal A (40/82,48.78%), Luminal B (8/82,9.76%), HER2+ (12/82,14.64%), TNBC (22/82,26.82%) with mean age 55.88 ±14.01 for Luminal A (LA), 64.7 ±13.26 for Luminal B (LB), 59.17 ±9.86 for HER2+ and 53.18 ±11.17 for TNBC. Histologically grade I cancer was found in 29.27% cases, grade II in 39.02%, and grade III in 31.71% cases. Regarding the results comparing the pathological variable among the four tumor subtypes (Table 3), tumor histological grade was significantly different among them. The percentage of histological grade 3 in LA (10%) was quite low as compare to LB (62.5%), HER2+ (50%), and TNBC (50%). All breast cancers histological types were as follows: invasive ductal carcinoma (IDC,n=74), invasive lobular carcinoma (ILC,n = 4), mucinous carcinoma (n= 2), medullary carcinoma (n=2).

Regarding MRI features (Table 4),all tumors were detected as an area of abnormal enhancement. The majority of the lesions in LA and TNBC subtype showed mass-like enhancement 38/40(95%) in LA,18/22(81.82%), in TNBC, as compared to 4/8(50%)for LB and 7/12(58.33%) for HER2+ with p=0.0023. On DCE MRI larger tumor size was found in LB subtype, 45.88±14.3mm in LB Vs. 40.67±8.91mm

in HER2+, 38.82±8.47mm in TNBC, and 30.95±13.01mm in LA respectively with p=0.0016. Most of the LA (84.21%), (Figure 1) and TNBC (68.18%) tumors were unifocal as compare to HER2+ (41.67%) and LB (50%) with p=0.0002. Intratumoral necrosis was more common in LB (62.5%), HER2+ (58.33%) and TNBC (54.55%) as compare to LA (20%) with p=0.0072. Most of the TNBC with mass-like enhancement had oval shape (44.44%),p=0.006 while 100% of LB, 100% of HER2+, and 71.05% of LA had irregular shapes. The margins of the TNBCs subtype were smooth (55.56%), p<0.0001 as compared to LA (68.42%) which were mainly spiculated. The predominant internal enhancement of the TNBC was rim enhancement, identified in (55.56%), p<0.0001, while heterogeneous internal enhancement was predominant in LB (Figure 2), HER2+ (Figure 3) and LA subtypes, 100%, 85.71%, and 68.42% respectively. No statistically significant difference was found regarding the distribution and internal enhancement of non-mass like cancer among the different subtypes, p=0.27.The intratumoral high signal intensity on unenhanced fat-suppressed T2-weighted images was identified in 16/22(72.73%) of TNBCs (Figure 4) which correspond to morphologically and pathologically intratumoral necrosis, as compared to 8/40(20%), 2/8(25%), 3/12(25%) in LA, LB and HER2+subtypes, p=0.0003. No significant difference was identified

Table 2: Classification of Molecular subtype by Receptor Status

Subtype	Receptor Status
Luminal A	ER- and / or PR- positive and Ki 67<14 %
Luminal B	HER 2 negative subtype: ER - and / or PR Positive with (Ki67>14%) and HER2 Negative.
	HER 2 positive subtype: ER-and /or PR positive with HER 2 positive.
HER2+	ER Negative and PR negative , HER2 positive
TNBC (basal)	ER Negative PR Negative, and HER2 Negative

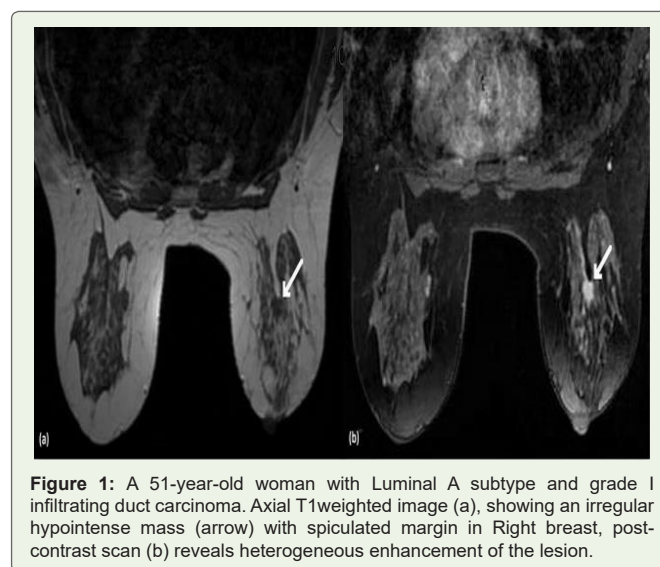


Figure 1: A 51-year-old woman with Luminal A subtype and grade I infiltrating duct carcinoma. Axial T1weighted image (a), showing an irregular hypointense mass (arrow) with spiculated margin in Right breast, post-contrast scan (b) reveals heterogeneous enhancement of the lesion.

Table 3: Histopathologic data of patients with LA, LB, HER2+, and TNBC breast cancer subtypes

Histopathological Features	Tumor subtype				p value	
	LA (N=40)	LB (N=8)	HER2+ (N=12)	TNBC (N=22)		
Age in years (mean ± SD)	55.88±14.01	64.75±13.26	59.17±9.86	53.18±11.17	0.14	
Histological Grade	1(Low)	21(52.5%)	0(0%)	0(0%)	0.00012	
	2(Intermediate)	15(37.5%)	3(37.5%)	6(50%)		
	3(High)	4(10%)	5(62.5%)	6(50%)		11(50%)
Histological Type	IDC	37(92.5%)	7(87.5%)	12(100%)	18(81.82%)	0.11
	ILC	3(7.5%)	1(12.5%)	0(0%)	0(0%)	
	Medullary	0(0%)	0(0%)	0(0%)	2(9.09%)	
	Mucinous	0(0%)	0(0%)	0(0%)	2(9.09%)	

among the Time-intensity curve analysis among different subtypes, $p=0.074$. The visual detectability of the different subtypes at DWI was not significantly different among tumor subtypes. ADC values were significantly different among tumor subtypes, $p=0.017$, the mean ADC value of TNBC was $1.28 \pm 0.23 \times 10^{-3} \text{mm}^2/\text{s}$ which was higher than that of LA ($1.153 \pm 0.25 \times 10^{-3} \text{mm}^2/\text{s}$), LB ($1.04 \pm 0.13 \times 10^{-3} \text{mm}^2/\text{s}$) and HER2+ ($1.14 \pm 0.18 \times 10^{-3} \text{mm}^2/\text{s}$).

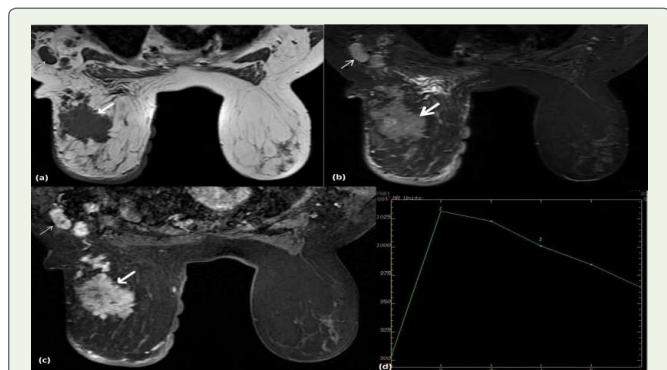


Figure 2: A 69-year-old woman with Luminal B subtype and grade II infiltrating duct carcinoma. Axial T2 (a) and T2 FAT SAT (b) images show an irregular mass lesion with spiculated margin (thick arrow) in left breast along with adjacent multifocal lesions, axillary adenopathy (thin arrow), skin and prepectoral edema, post-contrast scan (c) heterogeneous enhancement of the lesion with type III curve (d) seen.

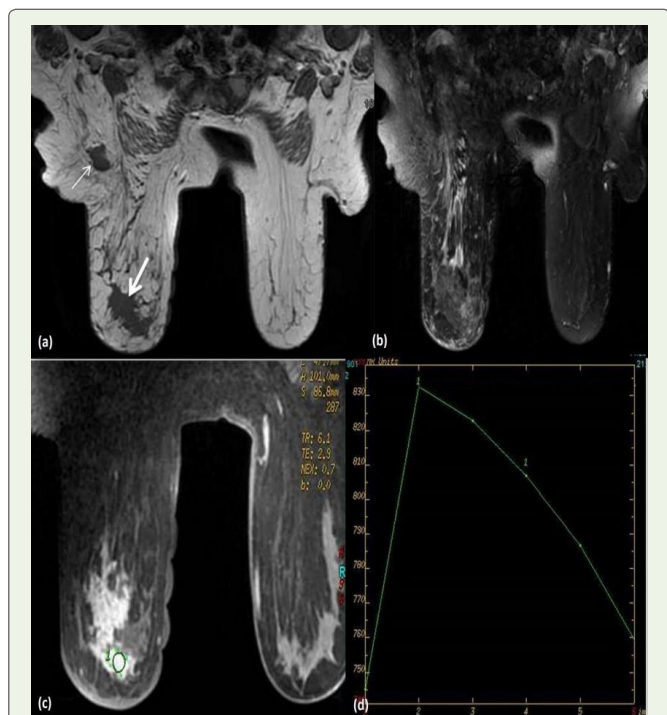


Figure 3: 52-year-old women with HER2+ subtype and grade III infiltrating duct carcinoma. (a) T1 WI showing an irregular hypointense mass lesion with spiculated margin in the left breast (thick arrow) along with axillary lymphadenopathy (thin arrow), (b) T2 FAT SAT image reveals perilesional, prepectoral and skin edema, post-contrast scan (c) shows heterogeneous enhancement of the lesion with (d) Type III curve.

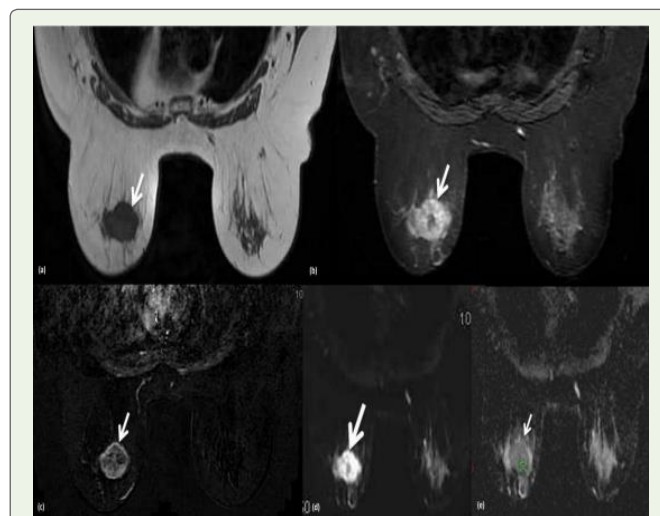


Figure 4: 68-year-old women with TNBC subtype and grade II infiltrating duct carcinoma. T1 (a) hypointense, T2 FAT SAT (b) image shows a hyperintense oval lesion with smooth margin (arrow) in the left breast, post-contrast subtraction image (c) reveals peripheral rim enhancement, DWI image (d) with ADC map (e) showing peripherally restricted diffusion with high ADC values ($1.23 \times 10^{-3} \text{mm}^2/\text{s}$).

Among the associated features (Table 5) axillary adenopathy was more common in LB (87.5%) as compared to HER2+ (66.67%), TNBC (36.36%), and LA (15%) with $p=0.0001$. Skin, perilesional and prepectoral edema were more common in LB (75%) and HER2+ (58.33%) as compared to TNBC (18.18%) and LA (7.5%).

Discussion

Breast cancer with different molecular subtypes has a different pattern of initial disease presentation and metastatic spread. Different subtypes respond differently to radiation and chemotherapy [8,9]. Our study may help in guiding different MRI features helpful in diagnosing molecular subtypes of breast cancer, which would further improve the potential for presurgical personalized medical care.

In our study, we could not find significant age differences among different subtypes as compared to previous study conducted by Osman NM et al where it was found that TNBC was more common at a younger age (43.1 ± 8.2) as compared to ER (45 ± 6.1) and HER2+ (47.4 ± 6.6) [10].

The present study showed that histologically high grade tumors were more common in LB, HER2+ and TNBC subtypes as compared to LA which was consistent with previous studies conducted by Lacroix BM et al and Uematsu T et al. [11,25]

Luminal A tumors were more common in our study (48.78%), with histological grade I (52.5%), presenting as a mass lesion with an irregular shape, spiculated margin, and heterogeneous enhancement along with type III curve. These observations were similar to the study conducted by Youk JH et al [26]. Overall, Luminal A breast cancer is associated with the most favorable prognosis, with a 5-year survival rate of more than 80%. This excellent prognosis is in part because the expression of the steroid hormone receptor is predictive of a favorable response to hormonal therapy [16,17,18].

Table 4: MRI features of different subtypes of Breast Cancer.

MRI Parameters	Tumor Subtype				p value
	LA (N=40)	LB (N=8)	HER2+ (N=12)	TNBC (N=22)	
T2-WI Signal intensity					
Low/Equal	32(80%)	6(75%)	9(75%)	6(27.27%)	0.0003
High/Very High	8(20%)	2(25%)	3(25%)	16(72.73%)	
DCE-MRI Tumor size (mm)	30.95±13.01	45.88±14.37	40.67±8.91	38.82±8.47	0.0016
Multifocality					
Yes	8(15.79%)	4(50%)	7(58.33%)	7(31.82%)	0.0002
No	32(84.21%)	4(50%)	5(41.67%)	15(68.18%)	
Presence of Necrosis					
Yes	8(20%)	5(62.5%)	7(58.33%)	12(54.55%)	0.0072
No	32(80%)	3(37.5%)	5(41.67%)	10(45.45%)	
Morphology					
Mass	38(95%)	4(50%)	7(58.33%)	18(81.82%)	0.0023
Non mass	2(5%)	4(50%)	5(41.67%)	4(18.18%)	
Mass shape					
Round	1(2.63%)	0(0%)	0(0%)	4(22.22%)	0.006
Oval	10(26.32%)	0(0%)	0(0%)	8(44.44%)	
Irregular	27(71.05%)	4(100%)	7(100%)	6(33.33%)	
Margin					
Smooth	3(7.89%)	0(0%)	0(0%)	10(55.56%)	<0.0001
Irregular	9(23.68%)	2(25%)	1(14.29%)	5(27.78%)	
Spiculated	26(68.42%)	2(50%)	6(85.71%)	3(16.67%)	
Internal enhancement					
Homogeneous	10(26.32%)	0(0%)	0(0%)	2(11.11%)	<0.0001
Heterogeneous	26(68.42%)	4(100%)	6(85.71%)	6(33.33%)	
Rim	2(5.26%)	0(0%)	1(14.29%)	10(55.56%)	
Non-Mass distribution					
Segmental	2(100%)	1(25%)	2(28.57%)	2(50%)	0.27
Regional	0(0%)	3(75%)	5(71.43%)	2(50%)	
Internal enhancement					
Homogeneous	0	0	0	0	~
Heterogeneous	2(100%)	4(100%)	5(100%)	4(100%)	
Clumped	0	0	0	0	
Kinetic curve					
I	1(2.5%)	0(0%)	0(0%)	3(13.64%)	0.074
II	7(17.5%)	1(12.5%)	1(8.33%)	5(22.73%)	
III	32(80%)	7(87.5%)	11(91.67%)	14(63.64%)	
DW-MRI					
ADC(mean value x 10 ⁻³ mm ² /s)	1.153±0.25	1.04±0.13	1.145±0.18	1.28±0.23	0.017

Table 5: Associated MRI finding of Breast Cancer Subtypes.

Findings	L A (40)	LB (8)	HER2+(12)	TNBC (22)	p value
Skin or nipple invasion	3(7.5%)	1(12.5%)	1(8.33%)	1(4.55%)	0.018
Chest Wall or Pectoralis muscle invasion	1(2.5%)	1(12.5%)	1(8.33%)	1(4.55%)	0.087
Edema					
Absent	34(85%)	2(25%)	3(25%)	18(81.82%)	<0.0001
Perilesional	4(10%)	6(75%)	7(58.33%)	2(9.09%)	<0.0001
Skin	3(7.5%)	6(75%)	7(58.33%)	2(9.09%)	<0.0001
Perilesional+ Skin	4(10%)	6(75%)	7(58.33%)	1(4.55%)	<0.0001
Perilesional + Prepectoral	4(10%)	6(75%)	9(75%)	3(13.64%)	<0.0001
Perilesional+ prepectoral +skin	3(7.5%)	6(75%)	7(58.3%)	4(18.18%)	<0.0001
Axillary adenopathy	6(15%)	7(87.5%)	8(66.67%)	8(36.36%)	<0.0001
Architectural Distortion	2(5%)	2(25%)	3(25%)	4(18.18%)	0.010

Grimm et al. and Agarwal G et al. reported that multicentric or multifocal disease was significantly more frequent in Luminal B and HER2 positive tumors. These tumors were also associated with axillary adenopathy, skin, perilesional, and prepectoral edema as compared to LA and TNBC which indicate a more invasive behavior and greater metastatic potential. The present study also shows similar observations. Perifocal edema can often be detected around tumors which are mainly caused by the immunohistopathologic response of the body against tumors through emitting cytotoxic T-Cells natural killer cells and macrophages. Tumor-associated macrophages (TAM) are known to induce tumor angiogenesis by emitting vascular endothelial growth factor. Prepectoral edema may be explained pathophysiologically through the anatomy of the lymphatic drainage pathway, indicating a possible correlation between prepectoral edema and lymphatic spread. Blocked lymphatic trails and nodes could be responsible for some sort of lymphatic obstruction within the breast and explain the formation of pectoral edema [19, 20, 22].

HER2 nue overexpression may be linked with overall increased tumor viability and a significant increase in the population of visible hypoxic cells, leading to hypoxia inducible factor-2 alpha overexpression which is related to high metastatic potential. Identification of multifocal disease in the breast is important because these findings may represent contradictions to breast conservation therapy. Four (33.3%) of our HER2+ cases and two of LB (25.9%) with HER2 enrich had microcalcification on mammography. It is mentioned in the literature that calcification is encountered in majority of HER 2 positive cancer whereas it is uncommon in triple-negative breast cancer [21, 22].

TNBC showed a high T2 signal intensity (72.73%) and rim enhancement (55.54%) in our series as compared to 71.4% and 61.6% in the study conducted by Osman NM et al. The hyperintense signal corresponded to intratumoral necrosis, which is a prognostic factor in invasive breast cancer. It is reported that the presence of moderate to marked central tumoral necrosis decreases relapse-free survival and increases mortality in both patients with node-negative and node-positive disease. Centrally necrotizing breast cancers were characterized by early systemic metastasis and an accelerated clinical course [10,25].

Two TNBC were hyperintense on T2WI without necrosis, their histopathological analysis revealed that they were mucinous carcinoma and was similar to the study of Osman NM et al. Uematsu et al reported that 66% of TNBC were unifocal in contrast to 81.82% in our study [25] Two medullary carcinomas were also of TNBC subtype which is in agreement with previous study [25]. Two patients of TNBC were BRACA I positive. One had associated ovarian malignancy with hepatic and peritoneal metastasis.

TNBC subtype had high ADC value (1.28 ± 0.23) as compared to other subtypes may be due to tumor necrosis causing increase diffusion and higher ADC value, another explanation for increased ADC value is that in ER positive tumors the ADC value becomes less than in ER-negative as the estrogen receptors inhibit the tumor angiogenesis decreasing perfusion and thus affecting the ADC value [26-29].

In conclusion, MR imaging helps diagnose Luminal A tumors which present as a mass with an irregular shape, spiculated margin, and heterogeneous enhancement. TNBC presents several MRI predictors on DCE-MRI such as unifocal, rim enhancing mass with round or oval shape, smooth margin, center high signal intensity on T2 weighted images, and higher ADC values on DWI. A multifocal or non-mass lesion with lymph node involvement, skin, peritumoral and prepectoral edema are more common in Luminal B and HER2 molecular subtypes breast cancer.

Strength and Limitation: We have taken different types of edema patterns as well as ADC values of the tumors in the study along with their morphological features on MR imaging which further helps in the characterization of different molecular subtypes. This study has less number of Luminal B and HER2+ subtype breast cancer. Further studies are needed to see the specific pattern in these subtypes.

References

1. Trap I, Le Blanc SM, David J Lalonde L, Tran- Thanh D, Labelle M, et al (2014) Molecular classification of infiltrating breast cancer: toward personalized therapy. *Radiographics* 34:1178-1195.
2. Dogan BE, Turnbull LW (2012) Imaging of triple-negative breast cancer. *Annals of Oncology* 23 :23-29.
3. Kimbery H. Allison (2012) Molecular Pathology of Breast Cancer: What a Pathologist Needs to know *Am J ClinPathol* 138: 770-780.
4. Simpson PT, Reis-Filho JS, Gale T, Lakhani SR (2005) Molecular evolution of breast cancer. *J Pathol* 205: 248-254.
5. Almir GV Bitencourt, Nara P Pereira, Luciana K L Franca, Caroline B Silva, Jociana Paludo (2015) Role of MRI in staging of breast cancer patient: does histological type and molecular subtype matter? *Br J Radiol* 88: 20150458.
6. Carl J. D'Orsi, Edward A. Sickles, Ellen B. Mendelson & Elizabeth A. Morris. *ACRBI-RADS Atlas. Breast Imaging Reporting and Data System 5th Edition* 2013.
7. Plaza MJ, Handa P, Esserman LE (2017) Preoperative MRI evaluation of axillary lymph nodes in invasive ductal carcinoma: comparison of luminal A versus luminal B subtypes in a paradigm using ki67 and receptor status. *AJR* 2017 208: 910-915.
8. Park SH, Moon WK, Cho N, In Chan Song C, Changet JM et al (2010) Diffusion - weighted MR Imaging : pretreatment prediction of response to neo adjuvant chemotherapy in patient , with breast cancer *Radiology* 257: 56-63.
9. Trop I, LeBlanc SM, David J, LucieLalonde, DaMaude Labelle et al (2014) Molecular classification of Infiltrating Breast Cancer: Towards Personalized therapy. *Radiographics* 34: 1178-1195.
10. Osman NM, Nivinei C, AbdRaboh NM (2014) Triple negative breast cancer: MRI features in comparison to other breast cancer sub types with correlation to prognostic pathologic factors. *The Egyptian Journal of Radiology and Nuclear medicine* 45: 1309-1316.
11. M BoisserieLacroix, G Mac Grogan, M Debled, S Ferron, M Asad- Syed, et al (2012) Radiological features of triple – negative breast cancers (73 cases). *Diagnostic and interventional Imaging* 93:183-190.
12. Chen JH, Agrawal G, Feig B, H-M Baek, P M Carpenteret PM et al (2007) Triple – Negative breast cancer: MRI features in 29 patients. *Ann oncol* 12: 2042-2043.
13. Jeon- Hor Chen, Hyun- Man Baik, Orhan Nalioglu, Min Ying Su (2008). Estrogen Receptor and Breast MR Imaging Features. A correlation study. *J Magn Reson Imaging* 27: 825-833.
14. M BoisserieLacroix, G Hurteventlabrot, S Ferron, N Lippa, H Bonnefoi, et al (2013) Correlation between imaging and molecular classification of breast cancers. *Diagnostic and interventional imaging* 94: 1069-1080.

15. SenJiang, You-Jia Hong, Fan Zhang, Yang- Kang Li (2017) Computer aided evaluation of the correlation between MRI Morphology and immune histochemical biomarkers or molecular sub types in breast cancer. *Sci Rep* 7: 13818.
16. C Aliti, E Pages, F curror Doyon , H Perrochia, I Millet, P Taourel (2014) Correlation between MR imaging prognosis factors and molecular classification of breast cancers. *Diagnostic and Interventional imaging* 95: 235-242.
17. S Rashmi, S Samala , S Sudha Murthy, Kotha S, Rao YS, et al (2018) Predicting the molecular sub type of breast cancer based on mammography and ultrasound findings *IJRI* 28: 354-361.
18. Costantini M, Belli P, Distefano D, Bui E, Matteo MD, et al (2012) Magnetic resonance imaging feature in triple negative breast cancer: comparison with luminal and HER 2 over expressing tumors. *Clin Breast cancer* 12: 331-339.
19. Wang Y, Narasimhan B, Longacre TA, Bleicher RJ, Sunita Pal (2008) Estrogen receptor – negative invasive breast cancer: Imaging features of tumors with and without human epidermal growth factor receptor type II over expression. *Radiology* 246: 367-375.
20. J Sutton E, Dashevsky BZ, Hun Oh J, Veeraraghavan H, Apte AP (2016). Breast cancer molecular sub type classifier that incorporates MRI features. *J Magn Reson Imaging* 44: 122-129.
21. Agarwal G, Chen JH, Back HM, Hsiang D, Mehta RS (2007) MRI features of breast cancer: a correlation study with HER 2 receptor *Annals of oncology* 18: 1903-1907.
22. Grimm LJ, Johnson KS, Marcom PK, Baker JA, Mary S Soo(2014) Can breast cancer molecular sub type help to select patient for preoperative MR Imaging? *Radiology* 274: 352-358.
23. Sung J S, Jochelson MS, Breman S, Joo S, Wen YH et al (2013) MR Imaging features of triple negative breast cancer *Breast J* 19: 643-649.
24. Krizmanich – Connif K, Paramagul C, Patlerson SK, Helvie MA, et al (2012) Triple receptor- Negative breast cancer: Imaging and clinical characteristics *198:458-464*.
25. Uematsu T, Kasami M, Yuen S Triple- Negative breast cancer: correlation between MR Imaging and Pathologic findings . *Radiology* 250: 638-647.
26. Youk JH, Son EJ, Chung J, Kim JA, Kim EK (2012) Triple – negative invasive breast cancer on dynamic contrast enhanced and diffusion – weighted MR imaging comparison with other breast cancer subtypes . *Eur Radiol* 22: 1724-1734.
27. Martincich L, Deantoni V, Bertotol, Redana S , Kutatzki F, et al (2012) Correlation between diffusion – Weighted imaging and breast cancer biomarkers. *European Radiology* 22: 1519-1528.
28. Kim SH, Cha ES, Kim HS, Kang BJ, Choi JS, et al (2009) Diffusion weighted imaging of breast cancer: correlation of the apparent diffusion coefficient value and prognostic factors. *J Magn. Reson. Imaging* 30: 6 15-620.
29. Dogan S, Ozman S, Oz B, Imamoglu H, Kabrman G (2018). Comparison of different Dynamic contrast enhanced Magnetic Resonance Imaging Descriptors and clinical findings Among Breast Cancer subtypes Determined Based on molecular Assessment. *Iranian Journal of Radiology* September 15: 64889.